POLITECNICO
MILANO 1863

DIPARTIMENTO DI MECCANICA

mecc

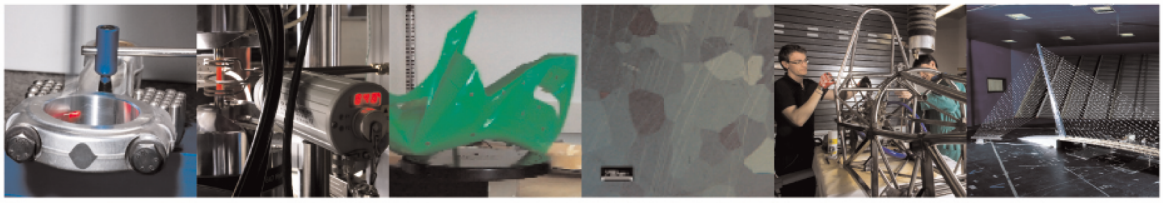

Optimized Design and Characterization of a Non-Linear 3D Misalignment Measurement System

Davide Maria Fabris, Alice Meldoli, Paolo Salina, Remo Sala, and Marco Tarabini

This is a post-peer-review, pre-copyedit version of an article published in *IEEE Transactions on Instrumentation and Measurement*. The final authenticated version is available online at: https://dx.doi.org/10.1109/TIM.2022.3152312

DIPARTIMENTO DI MECCANICA ■ POLITECNICO DI MILANO
via G. La Masa, 1 ■ 20156 Milano ■ EMAIL (PEC): pecmecc@cert.polimi.it
http://www.mecc.polimi.it
Rev. 0

Optimized design and characterization of a non-linear 3D misalignment measurement system

Fabris D. M.[1], *Student Member, IEEE*, Meldoli A.[2], *Student Member*, *IEEE*, Salina P.[3], Sala R.[4] and Tarabini M.[5], *Senior Member, IEEE*

***Abstract*— This work proposes a framework for the optimization of the metrological performances of a system that measures the relative position and orientation between two surfaces. The method is based on the creation of a non-linear measurement model of the instrument. The method uses the Monte Carlo method and the Design of Experiments techniques for determining the instrument uncertainty and the uncertainty sensitivity versus the geometrical and metrological instrument characteristics. The result of the proposed approach is a non-linear simplified numerical model of the measurement uncertainty and of the bias error components, that is used for the instrument design and compensation. A case-study related to a misalignment measurement system based on a universal joint is presented. The measurement uncertainty computed with the proposed method has been compared with the one obtained in fit-to-purpose experiments performed with a robotic manipulator. An optimal calibration procedure is then used in order to identify the parameters of the system minimizing the overall uncertainty.**

***Index Terms*—Design of Experiments, GUM, Metrology, Monte Carlo Method, Robotics, Uncertainty.**

I. Introduction

In the industrial field, sensors are employed to measure quantities for control, quality, and safety purposes. The result of a measurement process is composed by the estimate of the measurand and by the measurement uncertainty [1], [2], that are positional and dispersion indicators of the process itself. The de facto reference for the expression of the measurement uncertainty is the International Organization for Standardization (ISO) – International Electrotechnical Commission (IEC) – International Organization of Legal Metrology (OIML) – The International Bureau of Weights and Measures (BIPM) Guide to the expression of Uncertainty in Measurement (GUM) [3]–[7]. The formulation of the uncertainty analysis developed by the GUM is established upon the Theory of Probability (TP) [8]–[11].

The minimization of the measurement uncertainty is usually achieved during the sensor's design phase, either via physical prototypes or virtual instrument models [7]. Nuccio [12] proposed both a numerical and an approximate theoretical method for estimating the uncertainty of virtual instrument models. Locci et al. [13] focused on the metrology of a generic digital signal processing (DSP)-based measurement system to characterize the performance of a power system. Caldara et al. [14] compared numerical and experimental approaches to evaluate the uncertainty of PC-based virtual instruments.

Several studies are founded on the GUM [4] and its supplements [5], [6]. Supplement 1 [5] deals with the propagation of distributions with the Monte Carlo Method (MCM). Supplement 2 [6] extends the GUM formulation to multi-output measurement systems. These methodologies exploit the MCM for estimating the uncertainty deriving from the Probability Distribution Functions (PDF) of the input variables. By means of the MCM, Battista et al. [15] characterized the uncertainty of a sound localization sensor, based on interaural time difference. Chen [16] evaluated the measurement uncertainty of a perspiration measurement system both via the GUM and through the MCM approach, gathering compatible results. Cox [17] provided guidance on the optimization of the MCM approach for evaluating uncertainty and expanded uncertainty, identifying its pitfalls and indicating means for validating the results. Sładek [18] presented the conception, the implementation and the validation of MCM-based procedure for evaluating the measurement uncertainty of Coordinate Measuring Machines (CMM). In fact, the applicability of the MCM in uncertainty characterization is testified by the abundant related literature [19]–[21].

An alternative formulation for the propagation and the quantification of measurement uncertainty is represented by the possibilistic approach. This framework is based on the Theory of Evidence (TE), as opposed to the Theory of Probability. Consistent scientific contribution within this field was produced

This paper was submitted for review on XX. This work was founded by Giorgi Engineering s.r.l.

[1] Davide Maria Fabris is with Politecnico di Milano, Mechanical Engineering Department, Via La Masa 1, 20156 Milan, Italy (email: davidemaria.fabris@polimi.it).

[2] Alice Meldoli is with Politecnico di Milano, Mechanical Engineering Department, Via La Masa 1, 20156 Milan, Italy (email: alice.meldoli@polimi.it).

[3] Paolo Salina is with Giorgi Engineering s.r.l., Via Papa Giovanni XXIII 51, 20090 Rodano, Italy (email: paolo.salina@giorgiengineering.it).

[4] Remo Sala is with Politecnico di Milano, Mechanical Engineering Department, Via La Masa 1, 20156 Milan, Italy (email: remo.sala@polimi.it).

[5] Marco Tarabini is with Politecnico di Milano, Mechanical Engineering Department, Via La Masa 1, 20156 Milan, Italy (email: marco.tarabini@polimi.it).

by Ferrero et al. [22]–[28] ranging from the theory of Random Fuzzy Variables (RFV) [22], [24], [25] to their application in the expression of measurement uncertainty [26], [27]. Researchers also focused on the comparison of methodologies based on TE and TP [23], [28].

When the target is the evaluation of uncertainty in Multi-Input Multi-Output (MIMO) non-linear measurement systems, both GUM and RFV approaches might become burdensome. In particular, the exploration of all the possible combinations of the measurement influencing factors becomes computationally expensive. Furthermore, the analysis of the process outputs becomes onerous, with the increase of the configurations to be compared. Moschioni et al. [29] proposed to combine the MCM with the Design of Experiments (DOE) [30] to overcome these limitations. The method identifies the factorial plane of the possible influence factors combinations to be processed by the MCM to identify a simplified uncertainty model describing how the measurement uncertainty depends on the influencing factors. The uncertainty propagation model of the measurement system is obtained through the DOE regression analysis. A systematic state of the art review evidenced limited scientific production on the subject [31]–[33].

Inspired by the work by Moschioni et al., this work focuses on the metrological characterization of MIMO non-linear measurement systems. The spotlight is set on the identification of the measurement model, on the regression of uncertainty propagation models, on the experimental assessment of uncertainty and on the measurement model calibration.

The paper is structured as follows. Section II reports the developed method. Section III details the application of the method on a case study. Section IV highlights the results of the work. In Section V, the conclusions are drawn, and further investigations are hypothesized.

II. Method

A. Measurement Model Identification

Vectorial quantities are considered to be column-wise arranged and are in bolded digits, functions are identified by the italic font. Matrices are reported with non-bolded capital letters.

Let us consider an ideal MIMO non-linear measurement system. The mathematical relationship among the N-dimensional input vector $\mathbf{X}$ and the M-dimensional output vector $\mathbf{Y}$ is described by the expression:

$$\mathbf{Y} = f(\mathbf{X}). \tag{1}$$

Where f is a non-linear function of $\mathbf{X}$, whose elements are the measured quantities and the disturbances.

B. Uncertainty Propagation Model Regression

The measurement model can be used to investigate the dependence of the uncertainty of $\mathbf{Y}$ from the uncertainty of the input variables contained in $\mathbf{X}$. In presence of function non-linearities it can be more convenient to adopt the MCM rather than the classical linearization described in the GUM. Furthermore, in order to systematically study the effect of the uncertainty on the elements of $\mathbf{X}$ on the element of $\mathbf{Y}$ it is possible to couple the DOE and the MCM as described in [29]. The procedure is schematically represented in Fig. 1. The DOE requires the identification of the number of Influence Factors (IF). Furthermore, all the influencing factors can assume only a fixed Number of Levels (NL). IF and NL identify a total Number of Combinations (NC) of the system's influence factors equal to NL^{IF}. The DOE generates a factorial space of analysis for performing the regression of models describing the system's uncertainty propagation laws. The MCM is applied to randomly sample the uncertainty PDF affecting each input variable for a predefined number of replicates (NR). Therefore, the MCM requires the selection of the PDFs, and the definition of the NR of the random sampling process.

For each of the NL^{IF} DOE configurations, the PDFs of the input variables are randomly sampled NR times. The total number of simulations is therefore $NR \cdot (NL^{IF})$. Sampled deviations from the nominal value are superposed to the input variables to obtain the perturbed inputs $\mathbf{X^*}_{i,j}$:

$$\mathbf{X^*}_{i,j} = \mathbf{X} + \boldsymbol{\delta}_{i,j}(\mathbf{U_X}). \tag{2}$$

Where vector $\boldsymbol{\delta}_{i,j}(\mathbf{U_X})$ represents the input perturbations as a function of the input uncertainties $\mathbf{U_X}$. Subscript i refers to the i-th configuration of the DOE, subscript j to the j-th random sampling of the MCM. For each i-th DOE configuration, the j-th perturbed input vector, $\mathbf{X^*}_{i,j}$, is fed to the system model, f, obtaining the corresponding perturbed output vector $\mathbf{Y^*}_{i,j}$. Subsequently, the propagated perturbations vector, $\mathbf{e}_{i,j}$, resulting from each j-th sampling process, is evaluated per each i-th DOE configuration. This is obtained by comparing the perturbed and the unperturbed output vectors:

$$\mathbf{e}_{i,j} = \mathbf{Y^*}_{i,j} - \mathbf{Y} = f(\mathbf{X^*}_{i,j}) - f(\mathbf{X}). \tag{3}$$

Measurement uncertainty is a combination of both the non-compensated bias errors components and random errors [1], [4]. The RMS of $\mathbf{e}_{i,j}$ over j leads to the identification of the Root Means Square Error, $\mathbf{RMSE}_i$, for each of the DOE configurations. The $\mathbf{RMSE}_i$ is used as a figure of merit for the quality of the measurement, and it accounts for both random and systematic error components.

$$\mathbf{RMSE}_i = [(\sum \mathbf{e}^2_{i,j}) / (NR-1)]^{1/2}. \tag{4}$$

The dependence of $\mathbf{RMSE}_i$ from the influencing factors can be derived by fitting MxN non-linear models to the resulting NL^{IF} configurations, obtaining the relation among $\mathbf{U_Y}$ and $\mathbf{U_X}$. The uncertainty of the output variables of the model, $\mathbf{U_Y}$, can be expressed as a function of the random components affecting input variables, $\mathbf{U_X}$:

$$\mathbf{U_Y} = s(\mathbf{U_X}). \tag{5}$$

Where s identifies the regressed non-linear uncertainty propagation model, $\mathbf{U_X}$ is the N-dimensional vector of the input

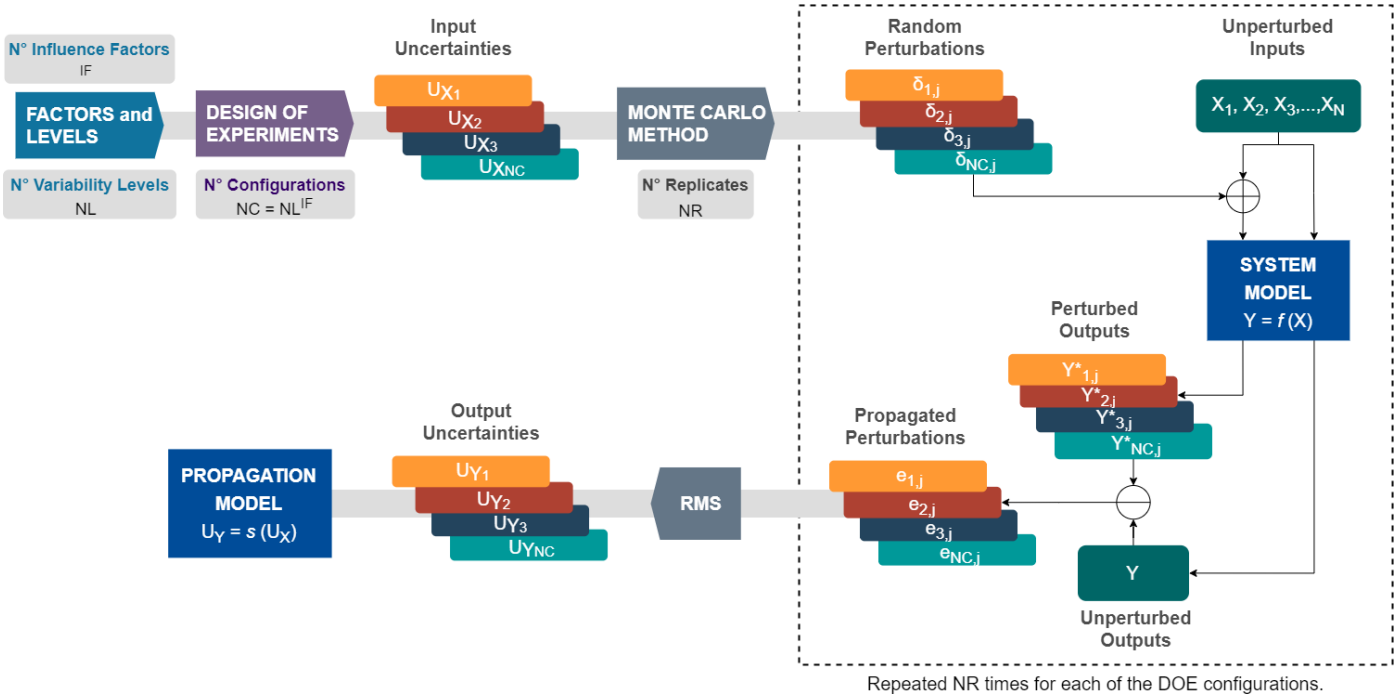

Fig. 1 - Schematic of the uncertainty propagation models regression. Each DOE configuration is sampled NR times by the MC method to perturb the system inputs. Perturbations of the i-th configuration are propagated through the system model. The RMS of the perturbations is calculated to obtain the output uncertainties. The model is then regressed considering the NL^{IF} configurations.

variables uncertainty, and $\mathbf{U}_Y$ is the M-dimensional vector of the output measurement uncertainty.

III. Case Study

The proposed method was applied to analyze the performances of a non-linear MIMO measurement system designed to monitor the 3D misalignments between two surfaces. The device is a 3D kinematic chain, composed by mechanically connected rigid bodies, as shown in Fig. *2*. Each of the six kinematic joints is sensed by either rotational or linear potentiometers, depending on its kinematics. Five sensors gauge rotations, one measures linear motion (q_3 in Fig. 2).

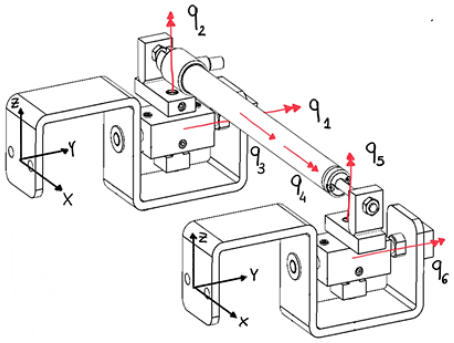

Fig. 2 - Schematics of the MIMO measurement system.

A. Measurement Model

In the MIMO non-linear measurement model, the measure is a function of the dimensions of the rigid bodies, **d**, of the instantaneous values of the measured Degrees Of Freedom (DOFs), **q**, and of the values of the DOFs in the zeroing condition, $\mathbf{q}_0$. In the measurement model identification, one of the two extremities was assumed to be grounded, the other was considered as movable. The subsequent composition of the three-dimensional transformations leading from the grounded reference system to the movable one resulted in the definition of the three-dimensional kinematic model. In general, three-dimensional transformations are represented through the homogeneous 3D pose matrix convention [34], [35]. Alternatively, their Euler formulation can be considered, provided that a convention is set on subsequent rotations. In the present study the xyz convention on rotations was selected. The 3D pose matrix H is a 4x4 squared matrix, in which R is the upper-left 3x3 rotation matrix and **T** is the upper-right 3x1 translation vector. The elements of the fourth row are zeroes, except for the rightmost one which is unitary. The equivalent Euler 3D pose **h** is a column vector, whose scalar components are the three translations and the three rotations with respect to the Cartesian axes, identified by subscripts x, y, and z. The following equation reports the two equivalent expressions.

$$H = [R \mid \mathbf{T}] \equiv \mathbf{h} = [T_x\ T_y\ T_z\ R_x\ R_y\ R_z]^{T}. \quad (6)$$

The measurement model of the system was derived by subsequently composing transformation matrices, resulting in the matrix leading from the fixed to the movable extremity.

$$H(\mathbf{q}_0, \mathbf{q}, \mathbf{d}) = \prod H_{r,r+1} \equiv \mathbf{h}(\mathbf{q}_0, \mathbf{q}, \mathbf{d}). \quad (7)$$

Where subscript r ranges from 1 to the number of reference systems that are considered in the kinematic chain derivation.

Each 3D homogeneous matrix $H_{r,r+1}$ depends on $\mathbf{q}_0$, $\mathbf{q}$ and $\mathbf{d}$. Consequently, the measurement model of the system is a 4x4 3D pose matrix, H, whose elements are non-linear functions of $\mathbf{q}_0$, $\mathbf{q}$, and $\mathbf{d}$. The Euler form, $\mathbf{h}$, was used since it allowed the direct definition of the translations' and of the rotations' values.

B. Uncertainty Propagation Model

The DOE-MCM allowed deriving a model for the measurement uncertainty $\mathbf{U_h}$, being the uncertainty, a vector composed by three translational components and three rotational ones. The model expresses the dependence of $\mathbf{U_h}$ from the sensors' uncertainties $\mathbf{U_q}$ and from the links dimension uncertainty $\mathbf{U_d}$. The latter are due to the deviation of the physical dimensions from the nominal dimension $\mathbf{d}$ and is supposed to be fully compensated during the calibration of the instrument. Its effect will be investigated in the experiments as a contribution of the calibration procedure.

In a first set of experiments, the influencing factors were set to the number of DOF of the system (i.e., 6). Test were then performed supposing that all the angular potentiometers are the same, and IF is equal to the number of different sensors mounted on the system (i.e., 2: linear and angular). Each IF assumed four levels (i.e., NL = 4), with values ranging from 0.001 to 1 mm or degrees, with a unitary step in $\log_{10}$ scale.

In the MCM, the number of replicates were imposed to one thousand (i.e., NR = 1000). The PDFs were assumed to be Gaussian for potentiometers and rectangular for encoders. Gaussian PDFs were generated by considering zero mean and standard deviation equal to the measurement uncertainties, $\mathbf{U_q}$. Rectangular PDFs were generated by considering zero mean and amplitudes equal to the least significant bit [1]. Table I summarizes the performed analyses. In each of the four configurations of Table I, for each i-th DOE configuration, the 3D kinematic model was applied to the j-th perturbed vector of coordinates defined as:

$$\mathbf{q}^*_{i,j} = \mathbf{q} + \boldsymbol{\delta}_{i,j}(\mathbf{U_q}). \quad (8)$$

TABLE I – PARAMETERS OF THE DOE AND MCM THAT WERE SELECTED FOR THE REGRESSION OF THE UNCERTAINTY PROPAGATION MODELS.

Influence Factors (IF)	Number of Levels (NL)	Probability Distribution Functions (PDFs)	Number of Replicates (NR)	Total runs
6	4	Gaussian	1000	4'096'000
6	4	Rectangular	1000	4'096'000
2	4	Gaussian	1000	16'000
2	4	Rectangular	1000	16'000

Where vector $\boldsymbol{\delta}_{i,j}$ represents the input measurements perturbation as a function of the input uncertainties $\mathbf{U_q}$, whose elements were obtained by randomly sampling the uncertainty PDFs. Then, $\mathbf{q}^*_{i,j}$ was fed to the measurement model, resulting in the corresponding perturbed output vector. The difference between the perturbed output, $\mathbf{h}^*_{i,j}$ and the unperturbed output, $\mathbf{h}$ is the error $\mathbf{e}_{i,j}$.

$$\mathbf{e}_{i,j} = \mathbf{h}^*_{i,j} - \mathbf{h} = \mathbf{h}(\mathbf{q}_0, \mathbf{q}^*_{i,j}, \mathbf{d}) - \mathbf{h}(\mathbf{q}_0, \mathbf{q}, \mathbf{d}). \quad (9)$$

As previously mentioned, under the hypothesis of the systematic errors not to be compensated, the RMS of $\mathbf{e}_{i,j}$ over index j captures the joint effect of random and systematic error sources. The uncertainty affecting the output variables, $\mathbf{U_h}$, is the RMSE of $\mathbf{e}_{i,j}$ and can be expressed as a function of the uncertainty affecting the input variables, $\mathbf{U_q}$:

$$\mathbf{U_h} = u(\mathbf{q}_0, \mathbf{U_q}, \mathbf{d}). \quad (10)$$

Where u identifies the regressed non-linear uncertainty propagation model, $\mathbf{U_q}$ is the N-dimensional vector of the input variables' uncertainties, and $\mathbf{U_h}$ is the M-dimensional vector of the output measurement uncertainties. The uncertainty propagation models provide the relation describing the impact that the sensors' uncertainty, $\mathbf{U_q}$, has on the uncertainty of the relative 3D pose measurement, $\mathbf{U_h}^{th}$. Under the non-linear hypothesis, the models were chosen to be second-order ones, their general expression is:

$$\mathbf{U_h}(\mathbf{q}_0, \mathbf{U_q}, \mathbf{d}) = A(\mathbf{q}_0, \mathbf{d})\cdot\mathbf{U_q}^2 + B(\mathbf{q}_0, \mathbf{d})\cdot\mathbf{U_q} + \mathbf{c}(\mathbf{q}_0, \mathbf{d}). \quad (11)$$

The combined application of the DOE and of the MCM resulted in the regression of the instrument's non-linear uncertainty propagation models. Fig. 3 and Fig. 4 report the results obtained by considering two influence factors and four number of levels. The more general formulation, with six influence factors and four number of levels, provided a more detailed, though redundant, representation of the models. Hence, for the sake of conciseness, it was not reported. The distinction among the sensors' measuring principles (i.e., potentiometers and encoders) led to analogous results, the choice was then to unify their discussion.

Fig. 3 reports the contour plot of the T_x uncertainty component in logarithmic scale, as a function of the linear and rotational sensors' uncertainties. The foremost purpose of these uncertainty propagation models is their application in the sensors' selection during the design phase. This kind of analysis allows selecting the possible configuration granting the desired measurement uncertainty.

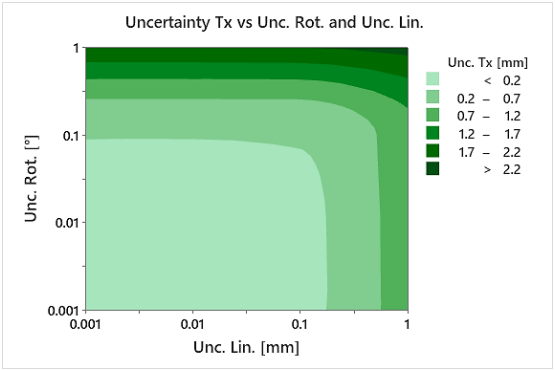

Fig. 3 - Representation of the mutual effect of the linear (Unc. Lin.) and rotational (Unc. Rot.) sensors' uncertainties on the 3D pose measurement translational component along the x axis (Unc. Tx).

Fig. 4 graphically depicts the sensitivity of the 3D pose measurement components. The left column shows the propagation model's coefficients for the translational components of the pose measurement, their rotational counterpart is shown in the right column. The influence of the uncertainty of rotational sensors is dominant, except for the T_x

element. In this case, both rotational and linear sensors contribute to the overall coordinate measurement uncertainty.

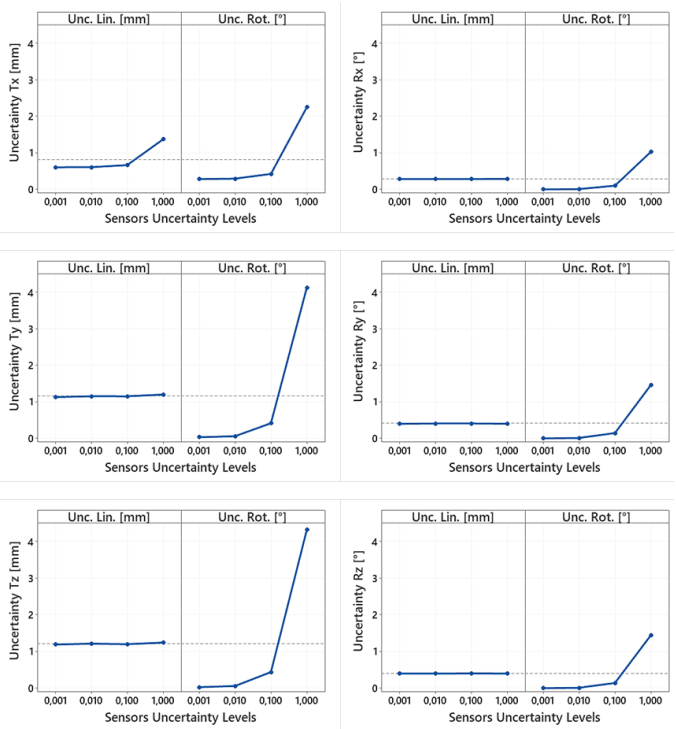

Fig. 4 - Translational uncertainties (Tx, Ty, Tz) as a function of the sensors' uncertainties (Unc. Lin., Unc. Rot.) - Rotational uncertainties (Rx, Ry, Rz) as a function of the sensors' uncertainties (Unc. Lin., Unc. Rot.).

C. Experimental Analysis and Model Calibration

Experiments were performed displacing the movable extremity of the measurement system using a Stäubli TX-60L anthropomorphic robot. Before performing the experiments, the robot was calibrated via laser tracking. The positioning accuracy resulted being equal to 0.1 mm within the considered working volume. After zeroing the sensors' readings in a predefined configuration, the movable extremity was displaced to reach NP predefined reference positions. These were identified by discretizing a cubic volume, with a side length of 50 mm. Twenty-seven points were defined by selecting the vertices of the cube, the midpoint of each face and side, plus the center point. The sensors' readings, $\mathbf{q}_p$ in each of the NP points were used to compute the 3D pose measurement, $\mathbf{h}$ ($\mathbf{q}_0$, $\mathbf{q}_p$, $\mathbf{d}$). The pose in correspondence of the cube centre, denoted by $\mathbf{h}(\mathbf{q}_0, \mathbf{q}_p^{\dagger}, \mathbf{d})$, was subtracted to every pose to compare the nominal motion imposed by the robot with the experimentally measured motion. The relative motions assigned to the device by the robot, $\Delta\mathbf{h}_p^{robot}$, was then compared to those measured by the system, $\Delta\mathbf{h}_p^{measured}$. The assessment of the uncertainty was carried out in terms of the RMS of each pose component. This led to the identification of the system's experimental uncertainty $\mathbf{U_h}$:

$$\mathbf{U_h} = [(\sum(\Delta\mathbf{h}_p^{measured} - \Delta\mathbf{h}_p^{robot})^2) /(NP-1)]^{1/2}. \quad (13)$$

As evidenced in equation (7), the 3D pose measurement depends on the physical dimensions $\mathbf{d}$, on the instantaneous sensors' readings, $\mathbf{q}$, and on their zeroing values $\mathbf{q}_0$. The instrument calibration can be used to determine the real sensitivities of the linear and of the rotational sensors, $\mathbf{s}$ and the real dimensions with an optimization procedure.

The quantity to be minimized was defined by considering the translational uncertainty U_T between the nominal motion by the robot ($\Delta\mathbf{h}_p^{robot}$) and the measured motion ($\Delta\mathbf{h}_p^{measured}$).

$$U_T(\Delta\mathbf{h}_p^{measured}, \Delta\mathbf{h}_p^{robot}) = (U_{Tx}^2 + U_{Ty}^2 + U_{Tz}^2)^{1/2}. \quad (14)$$

The optimization variables were subjected to the following physically informed constraints:

1. The physical dimensions $\mathbf{d}$, and the sensitivity update factors, $\mathbf{s}$, were imposed to be strictly positive.
2. The physical dimensions, $\mathbf{d}$, were allowed to vary by at most $\delta\mathbf{d}$, from their nominal values $\mathbf{d}^n$.
3. Given the symmetric nature of the system under analysis, the mirrored dimensions $\mathbf{d}_k$ and $\mathbf{d}_{k,D-k}$ were constrained in such a way that their values could at most differ by a predefined threshold, $\delta\mathbf{d}_{k,D-k}$.
4. The sensitivity update factors could either be optimized or they could be forced to be unitary, depending on the value of $\delta\mathbf{s}$. The sensitivity update factors calibration could be enabled separately.
5. The sensors' readings in the zeroing pose, $\mathbf{q}_0$, were allowed a variation, $\delta\mathbf{q}_0$, with respect to their nominal values $\mathbf{q}_0^n$.

The measurement model of the system could be calibrated within the considered working volume, given its initial formulation, the cost function to be minimized and the constraints of the optimization problem. Table II and Table III summarize the results of both the experimental uncertainty assessment and of the system model calibration. Table II details the subsequent definitions of the optimization problem, starting from the baseline in which the outcomes from the experimental assessment are provided. The identification of the physical dimensions and the symmetric constraint were enabled first, then the sensitivity update factors were introduced, eventually, the zeroing pose values were optimized. The cost function U_T variations is reported in the last column of Table II.

TABLE II – THE INCREMENTAL ENABLING OF CALIBRATION CONSTRAINTS AND THE CORRESPONDING VARIATIONS OF THE COST FUNCTION.

Calibration	$\delta\mathbf{d}_k$ [mm]	$\delta\mathbf{d}_{k,D-k}$ [mm]	$\delta\mathbf{s}_{lin}$ [-]	$\delta\mathbf{s}_{rot}$ [-]	$\delta\mathbf{q}_{0,lin}$ [mm]	$\delta\mathbf{q}_{0,rot}$ [°]	$\mathbf{U_T}$ [mm]
None	0.0	0.0	0.0	0.0	0.0	0.0	4.30
Dimensions	1.0	0.1	0.0	0.0	0.0	0.0	3.89
Dimensions Sensitivities	1.0	0.1	0.5	0.5	0.0	0.0	2.11
Dimensions Sensitivities Zeroing	**1.0**	**0.1**	**0.5**	**0.5**	**0.2**	**0.1**	**1.49**

The uncertainty values for each pose component are shown in TABLE III, bolded digits refer to the optimal calibration. FIG. 5 graphically represents the results obtained by means of the measurement model calibration. The discretized cube is shown,

together with both the nominal points reached by the robot and the corresponding points that were measured by the system.

TABLE III – RESULTS OF THE PERFORMED CALIBRATIONS. THE FIRST ROW REPORTS THE BASELINE, WITHOUT ANY CALIBRATION.

Calibration	U_{T_x} [mm]	U_{T_y} [mm]	U_{T_z} [mm]	U_{R_x} [°]	U_{R_y} [°]	U_{R_z} [°]
None	0.85	2.95	3.01	0.15	0.79	0.51
Dimensions	0.83	2.65	2.71	0.15	0.79	0.51
Dimensions Sensitivities	0.83	1.32	1.43	0.19	0.89	0.57
Dimensions Sensitivities Zeroing	**0.65**	**0.87**	**1.02**	**0.11**	**0.69**	**0.45**

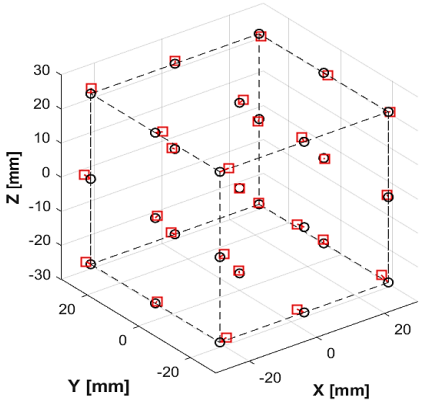

Fig. 5 - Depiction of the uncertainty assessment after the system model calibration. The discretized cube is represented by dashed lines, points reached by the robot are identified by black circles. The 3D points measured by the calibrated system are shown by means of red squares.

IV. DISCUSSION

The developed method allowed the analysis of the measure of a non-linear 3D misalignment measurement system. Prior to the successive analyses, the system underwent a redesign phase oriented at making its parameters more certain and defined. The mechanical structure was modified by inserting mechanical references for the mounting procedure, reducing the measurement bias. Elastic joints and ball bearings were introduced to ensure superior alignments and proper structural stiffness, diminishing the random error contributions.

The theoretical analysis led to the definition of the measurement model and to the regression of uncertainty propagation models. The regression models were obtained through the application of the joint DOE-MCM methodology. The models could be exploited while designing the system, depending on the specific application it is meant to work in. Namely, the a priori knowledge of the desired system precision ($\mathbf{U}_X$) can be translated into the required sensors' precision ($\mathbf{U}_Y$) by means of the derived non-linear model. The most adequate sensors typology and characteristics could then be properly selected. The metrological characteristics of the measurement model could also be assessed ex ante, through the graphical representation of the coverage regions of the propagated perturbances in Fig. 6, as per the GUM indications [5], [6].

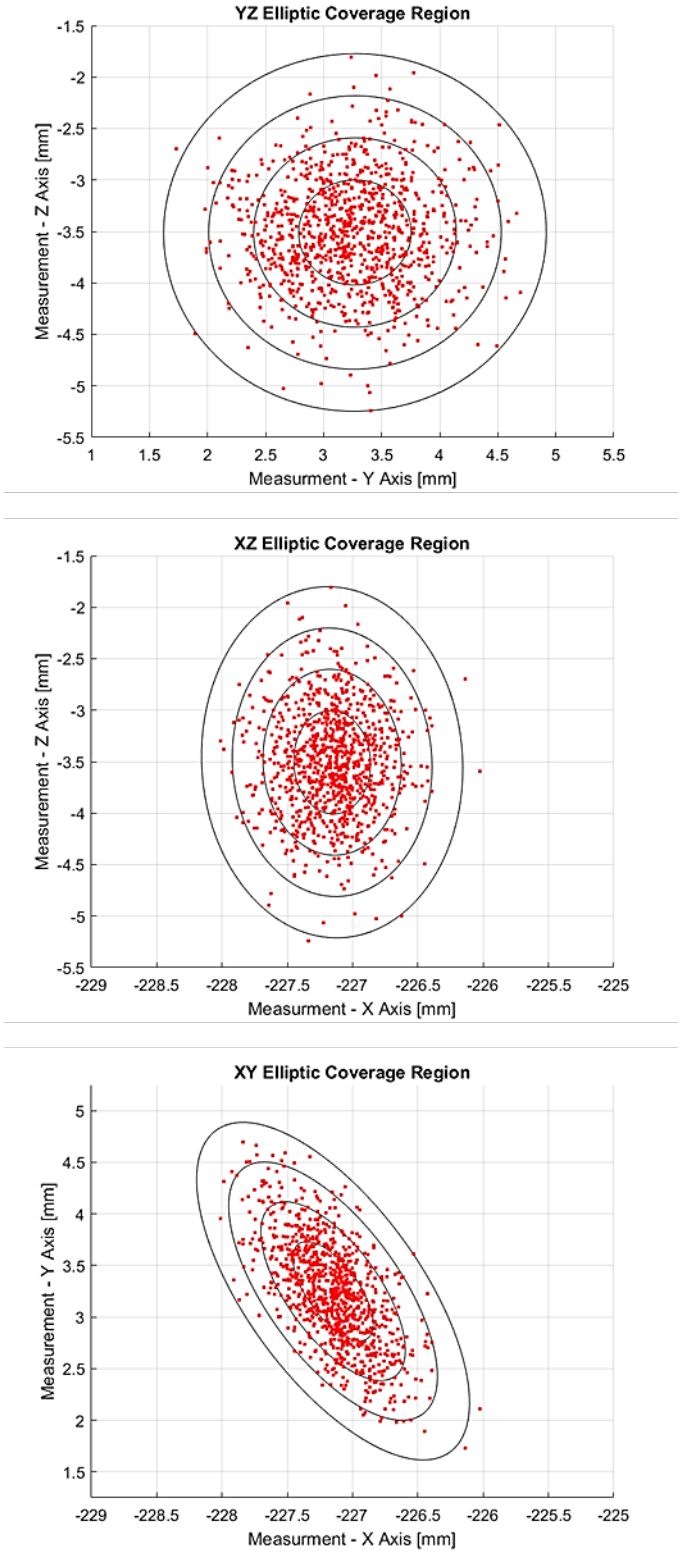

Fig. 6 - Elliptic coverage regions on XY, XZ and YZ planes. These distributions result from the propagation of the perturbed inputs via the measurement model of the system.

The possibility to design and optimize the system is of foremost importance, especially in the industrial field. The calibration procedure permitted the diminution of the systematic errors affecting the measurement. Hypothetically,

various measurement accuracies could be accomplished through the introduction of more and more strict requirements and procedures for the calibration process.

V. Conclusions

This work focused on the metrological characterization of a non-linear MIMO 3D misalignment measurement instrument. The measurement model was derived by analyzing the 3D kinematics of the instrument. Uncertainty propagation models were derived by the joint application of the Design of Experiments and of the Monte Carlo Method. The experimental uncertainty of the instrument was assessed by means of the implementation of a robotic manipulation procedure. The measurement model of the system was calibrated through an optimization routine.

Except for the robotic manipulation, which was implemented due to the very nature of the measurement instrument, the developed methods could be applied to other complex measurement chains. The joint application of the DOE and of the MCM could be enlarged by considering alternative solutions for designing the experiments, such as reduced order factorial analyses and Taguchi formulations. Further robotic manipulation procedures could be studied and developed in order to deepen the experimental characterization of the device. Furthermore, supplementary calibration routines could be investigated for the amelioration of the measurement model.

In conclusion, by relying on the information granted by both the uncertainty propagation models and the model calibration, the device could be re-designed so further to mitigate both random and systematic measurement error components.

Acknowledgments

Authors acknowledge Giorgi Engineering s.r.l. for financing the project and Innovative Security Solutions s.r.l. for granting the possibility to perform the robotic manipulation tests.

References

[1] E. O. Doebelin, *Measurement Systems: Application and Design*. 2004.

[2] H. W. Coleman and W. G. Steele, *Experimentation, Validation, and Uncertainty Analysis for Engineers*. 2018.

[3] Joint Committee for Guides in Metrology (JCGM), *Evaluation of measurement data – An introduction to the GUM and related documents*, no. July. 2009.

[4] Joint Committee for Guides in Metrology (JCGM), *Evaluation of measurement data — Guide to the expression of uncertainty in measurement*, vol. 50, no. September. 2008.

[5] Joint Committee for Guides in Metrology (JCGM), *Evaluation of measurement data – Supplement 1 to the "Guide to the expression of uncertainty in measurement" – Propagation of distributions using a Monte Carlo method*. 2008.

[6] Joint Committee for Guides in Metrology (JCGM), *Evaluation of measurement data – Supplement 2 to the "Guide to the expression of uncertainty in measurement" – Extension to any number of output quantities*, vol. 102, no. October. 2011.

[7] Joint Committee for Guides in Metrology (JCGM), *Guide to the expression of uncertainty in measurement — Part 6: Developing and using measurement models*. 2020.

[8] T. T. Soong, *Fundamentals of Probability and Statistics for Engineers*. John Wiley & Sons, Ltd, 2004.

[9] D. C. Montgomery, *Introduction to Statistical Quality Control*. John Wiley & Sons, Inc., 2009.

[10] D. C. Montgomery and G. C. Runger, *Applied Statistics and Probability for Engineers*, VII Ed., vol. 30, no. 1. John Wiley & Sons Inc., 2018.

[11] Joint Committee for Guides in Metrology (JCGM), *International Vocabulary of Metrology - Basic and General Concepts and Associated Terms (VIM)*, III Editio. 2008.

[12] S. Nuccio and C. Spataro, "Approaches to Evaluate the Virtual Instrumentation Measurement Uncertainties," *IEEE Trans. Instrum. Meas.*, vol. 51, pp. 1347–1352, 2002, doi: 10.1109/TIM.2002.808036.

[13] N. Locci, C. Muscas, L. Peretto, and R. Sasdelli, "A numerical approach to the evaluation of uncertainty in nonconventional measurements on power systems," *IEEE Trans. Instrum. Meas.*, vol. 51, no. 4, pp. 734–739, 2002, doi: 10.1109/TIM.2002.803290.

[14] S. Caldara, S. Nuccio, and C. Spataro, "Measurement Uncertainty Estimation of a Virtual Instrument," in *IEEE Instrumentation and Measurement Technology Conference*, 2000, doi: 10.1109/IMTC.2000.848724.

[15] L. Battista, E. Schena, G. Schiavone, S. A. Sciuto, and S. Silvestri, "Calibration and uncertainty evaluation using monte carlo method of a simple 2D sound localization system," *IEEE Sens. J.*, vol. 13, no. 9, pp. 3312–3318, 2013, doi: 10.1109/JSEN.2013.2272802.

[16] A. Chen and C. Chen, "Comparison of GUM and Monte Carlo methods for evaluating measurement uncertainty of perspiration measurement systems," *Meas. J. Int. Meas. Confed.*, vol. 87, pp. 27–37, 2016, doi: 10.1016/j.measurement.2016.03.007.

[17] M. G. Cox and B. R. L. Siebert, "The use of a Monte Carlo method for evaluating uncertainty and expanded uncertainty," *Metrologia*, vol. 43, no. 4, 2006, doi: 10.1088/0026-1394/43/4/S03.

[18] J. Sładek and A. Gąska, "Evaluation of coordinate measurement uncertainty with use of virtual machine model based on Monte Carlo method," *Measurement*, vol. 45, no. 6, pp. 1564–1575, Jul. 2012, doi: 10.1016/J.MEASUREMENT.2012.02.020.

[19] N. Locci, C. Muscas, and S. Sulis, "Modeling ADC nonlinearity in Monte Carlo procedures for uncertainty estimation," *Conf. Rec. - IEEE Instrum. Meas. Technol. Conf.*, vol. 1, no. 5, pp. 522–527, 2004, doi: 10.1109/IMTC.2004.1351102.

[20] E. Ghiani, N. Locci, and C. Muscas, "Auto-evaluation of the uncertainty in virtual instruments," *IEEE Trans. Instrum. Meas.*, vol. 53, no. 3, pp. 672–677, 2004, doi: 10.1109/TIM.2004.827080.

[21] G. Wubbeler, M. Krystek, and C. Elster, "Evaluation of measurement uncertainty and its numerical calculation by a Monte Carlo method," *Meas. Sci. Technol.*, vol. 19, p. 4, 2008, doi: 10.1088/0957-0233/19/8/084009.

[22] A. Ferrero and S. Salicone, "The Random-Fuzzy Variables: A New Approach to the Expression of Uncertainty in Measurement," *IEEE Trans. Instrum. Meas.*, vol. 53, no. 5, 2004, doi: 10.1109/TIM.2004.831506.

[23] A. Ferrero and S. Salicone, "A Comparative Analysis of the Statistical and Random-Fuzzy Approaches in the Expression of Uncertainty in Measurement," *IEEE Trans. Instrum. Meas.*, vol. 54, no. 4, p. 1475, 2005, doi: 10.1109/TIM.2005.851079.

[24] A. Ferrero and S. Salicone, "Fully Comprehensive Mathematical Approach to the Expression of Uncertainty in Measurement," *IEEE Trans. Instrum. Meas.*, vol. 55, no. 3, 2006, doi: 10.1109/TIM.2006.873799.

[25] A. Ferrero, M. Prioli, S. Member, S. Salicone, and S. Member, "Processing Dependent Systematic Contributions to Measurement Uncertainty," *IEEE Trans. Instrum. Meas.*, vol. 62, no. 4, 2013, doi: 10.1109/TIM.2013.2240097.

[26] A. Ferrero, M. Prioli, and S. Salicone, "Uncertainty propagation through non-linear measurement functions by means of joint Random-Fuzzy Variables," in *IEEE International Instrumentation and Measurement Technology Conference (I2MTC)*, 2015, doi: 10.1109/I2MTC.2015.7151540.

[27] A. Ferrero, M. Prioli, S. Salicone, and S. Member, "Joint Random-Fuzzy Variables: A Tool for Propagating Uncertainty Through Nonlinear Measurement Functions," *IEEE Trans. Instrum. Meas.*, vol. 65, no. 5, p. 1015, 2016, doi: 10.1109/TIM.2016.2514782.

[28] A. Ferrero, S. Salicone, and S. Member, "A Comparison Between the Probabilistic and Possibilistic Approaches: The Importance of a Correct Metrological Information," *IEEE Trans. Instrum. Meas.*, vol. 67, no. 3, p. 607, 2018, doi: 10.1109/TIM.2017.2779346.

[29] G. Moschioni, B. Saggin, M. Tarabini, J. Hald, and J. Morkholt, "Use of design of experiments and Monte Carlo method for instruments optimal design," *Meas. J. Int. Meas. Confed.*, vol. 46, no. 2, pp. 976–984, 2013, doi: 10.1016/j.measurement.2012.10.024.

[30] D. C. Montgomery, *Design and Analysis of Experiments*, IX Ed., vol.

106, no. 11. John Wiley & Sons Inc., 2017.
[31] M. Tarabini and A. Roure, "Modeling of influencing parameters in active noise control on an enclosure wall," *J. Sound Vib.*, vol. 311, no. 3–5, pp. 1325–1339, 2008, doi: 10.1016/j.jsv.2007.10.015.
[32] D. L. Hansen, "Design-of-Experiments and Monte-Carlo Methods in Upset Rate-Calculations," *IEEE Trans. Nucl. Sci.*, vol. 67, no. 1, 2020, doi: 10.1109/TNS.2019.2957656.
[33] D. M. Fabris, A. Meldoli, R. Sala, P. Salina, and M. Tarabini, "Metrological Characterization of Measurement Systems through Monte Carlo Simulations , Design of Experiments and Robotic Manipulation," *2021 IEEE Int. Work. Metrol. Ind. 4.0 IoT*, pp. 561–565, 2021, doi: 10.1109/MetroInd4.0IoT51437.2021.9488485.
[34] B. Siciliano, L. Sciavicco, L. Villani, and G. Oriolo, *Robotics: Modeling, Planning and Control*. Springer, 2009.
[35] B. Siciliano and O. Khatib, *Springer Handbook of Robotics*. 2016.

Davide Maria Fabris was born in Spilimbergo, Italy, in 1995. He received both the B.S. degree and the M.S. degree in Mechanical Engineering, from Politecnico di Milano, Milan, Italy, respectively in 2017 and in 2019. He is currently pursuing the Ph.D. in Mechanical Engineering at Politecnico di Milano, Milan, Italy.

His current research interests include advanced measurement systems, 3D computer vision, structured-light scanners for robotic guidance, and hyperspectral imaging.

Alice Meldoli was born in Milan, Italy, in 1995. She received both the B.S. degree and the M.S. degree in Mechanical Engineering, from Politecnico di Milano, Milan, Italy, respectively in 2017 and 2020. Since 2020 she is a Research Fellow at the Mechanical Engineering Department of Politecnico di Milano, Milan, Italy,

Her research focuses on computer vision and statistical analyses for industrial production monitoring.

Paolo Salina was born in Cernusco sul Naviglio, Italy, in 1972. He ideated and realized a three-dimensional misalignment measurement system for structural monitoring. He is co-holder of the system's patent. He is currently a lecturer at the Martesansa Formative Academy of Gorgonzola, Italy. He teaches Advanced Driver-Assistance Systems, focusing on measurement principles, calibration techniques and ADAS application on means of transport.

Remo Sala was born in Casatenovo, Italy, in 1961. He received the M.S. degree in Mechanical Engineering from Politecnico di Milano, Milan, Italy, in 1985. He received the Ph.D. in Mechanical Engineering, from Politecnico di Milano, Milano, Italy, in 1993.

His current research interests include advanced measurement systems for automation and robotics, 3D vision systems, both in the visible and in the infrared spectral domain. He is co-founder and president of Innovative Security Solutions s.r.l., a Spin Off of Politecnico di Milano's engineering 3D vision and robotic guidance devices for bin-picking applications. He is also co-founder of Steriline Robotics s.r.l., a Spin Off of Politecnico di Milano's developing a complete solution for the single-batch production of chemotherapeutic drugs.

Marco Tarabini (SM) was born in Lecco, Italy, in 1978. He received the M.S. degree in mechanical engineering and the Ph.D. (cum laude) in engineering of mechanical systems from the Politecnico di Milano, Lecco. He is currently Associate Professor of Mechanical and Thermal Measurement with Politecnico di Milano.

His current research focuses on the study of human body response to hand-arm and whole-body vibrations, algorithms for signal analysis for diagnostic purposes, the study of measurement uncertainty in industrial applications, and the design of measurement instruments for space applications.